Recognition and Prediction of Nonlinear Dynamic States of Microelectronic Devices Based on Machine Learning Algorithms

Xia Liu[1]*, Kangyi Wang[1], Chongguang Liu[2]
[1]School of Innovation and Entrepreneurship, North University of China, Taiyuan 030051, China
[2]Taiyuan Municipal Construction Group Co., LTD., Taiyuan 030000, China
E-mail: liuxia7681@163.com
*Corresponding author

Keywords: duffing oscillator, josephson knot, nonlinear dynamics, extreme learning machine

Received: April 11, 2024

The accurate identification and prediction of nonlinear dynamical states of microelectronic devices, especially Duffing vibrator systems, have become particularly important with the development of microelectronics technology. The complex dynamical behaviors of these systems pose a challenge to traditional analysis methods, and machine learning-based approaches provide an efficient and accurate new way to solve this problem. This paper presents a new state recognition system for the Duffing oscillator, designed using the extreme learning machine algorithm. The aim is to address the issues of large computation and limited detection accuracy associated with traditional recognition and detection methods. This paper also constructs a new detection system based on the noise precursor phenomenon of Josephson junctions. The results demonstrated that the constructed system had a recognition accuracy of 93.3% for the training set samples, a running time of 70 seconds, and better computational performance than traditional detection methods. The average accuracy of the Josephson junction bifurcation prediction system in detecting multiple bifurcation points was over 91%, with a maximum of 95%, which was more than 10 percentage points higher than traditional methods. The results of this paper have certain value in the field of nonlinear dynamic state detection of microelectronic devices, and can provide technical reference for the study of nonlinear dynamic equations of other devices.

Povzetek: Avtorji raziskujejo natančno identifikacijo in napovedovanje nelinearnih dinamičnih stanj mikroelektronskih naprav, zlasti Duffingovih vibratorjev. Uporabljajo pristop strojnega učenja za reševanje izzivov kompleksnega dinamičnega obnašanja teh sistemov.

1 Introduction

In microelectronic device research and development, accurately identifying and predicting nonlinear dynamical states is crucial for ensuring device performance and reliability. As microelectronics technology rapidly advances, device dynamical behaviors become increasingly complex, presenting challenges for traditional analytical methods [1]. Nonlinear dynamical state identification and prediction based on machine learning algorithms has become a powerful tool to solve this problem due to its efficiency and accuracy. Machine learning algorithms, especially deep learning models, have shown great ability to handle complex data and pattern recognition in several fields. In the analysis of nonlinear dynamics (NLD) of microelectronic devices, algorithms can learn from a large amount of experimental or simulation data to identify key features of the device behavior. This enables accurate prediction of its dynamic state. However, applying machine learning algorithms to identify and predict nonlinear dynamical states of microelectronic devices still presents challenges, such as data processing complexity, model selection, and optimization. In addition, how to ensure the consistency of the prediction results of the algorithms with the physical phenomena is also an important research issue [2-3]. The Duffing vibration system is an NLD model that has received great attention due to its widespread application in microelectronic devices. It can simulate the complex response of microelectronic devices under nonlinear forcing, including bi-stability, chaos, and periodic behavior [4]. The paper focuses on a machine learning algorithm-based method for state identification and prediction of Duffing vibrator systems. The objective of this study is to develop a machine learning algorithm-based model for the identification and prediction of NLD in microelectronic devices and to apply it to the analysis of Duffing vibrator systems.

Based on this background, this paper attempts to combine machine learning algorithms for identifying and detecting NLD states. The precise identification method of Duffing oscillator state based on extreme learning machine (ELM) and the detection method of Josephson junction bifurcation state have been constructed. The identification

of the traditional Duffing vibrator state mainly relies on calculating Lyapunov exponents. While these methods perform well on normalized speech data, they suffer from high computational volume and slow convergence. In practical applications, the proposed system improves upon the limitations of traditional methods by combining machine learning algorithms with microelectronic devices. The combination of machine learning algorithms and microelectronic devices enables the identification and prediction of nonlinear dynamical states of microelectronic devices. This is significant for the research and development of device dynamics. This manuscript is divided into four parts. The first part reviews the current research on NLD equations, Duffing oscillators, Josephson junctions, and ELM. The second part explains the implementation method of the new recognition and detection model. The third part combines the method proposed in the second part to conduct simulation experiments and analyze the results. The fourth part summarizes the conclusions of this paper.

2 Related works

With the development of research on non-linear differential equation (NLDE), various fields have begun to pay attention to the potential application of NLD in physical devices. In the study of microelectronic dynamics, Duffing oscillators and Josephson junctions have always been very popular research topics. Salas and Trujillo [5] accurately solved the NLDE of a one-dimensional, undamped, forced 3/5 Duffing oscillator using Weierstrass elliptic functions, obtaining the exact expression for its period. It showed the integrability of damped cubic Quintic equation, and explained the solution method for Duffing oscillator equation in the form of Mathematica code. Akilli et al. [6] applied predictable and deterministic periodic signals to the analysis of dynamic systems, enabling the detection of dynamic system states from time series data with deterministic processes. To detect signals of Duffing oscillators, wavelet scale was used as a quantitative indicator to draw wavelet scale index maps. These maps could detect weakening of the periodic signal of Duffing oscillators in a timely manner. By simulating and detecting weak periodic signals embedded in noise, the data showed that this method had a certain effect on Duffing state signal detection. This research on NLDE in the field of microelectronic devices was not limited to Duffing oscillators. Pernel Nguenang et al. [7] studied the Josephson junction and improved its nonlinear resonance phenomenon in oscillation through the NLDE system. They analyzed the various types of resonances in the Josephson junction using a multi-time scale method and obtained three types of resonance results. The steady-state solutions and stability of each type of resonance were evaluated. By integrating the equations of motion, the accuracy of NLDE system operation was verified, indicating that the dynamic state of Josephson junction will be strongly affected by the change of equation parameters.

In the study of NLD equations, Wu et al. [8] designed a new prediction method based on machine learning algorithms by integrating models of recurrent neural networks (RNNs). This prediction method could detect NLD states with uncertainty. After operating on the RNN model set, they used the Lyapunov exponent graph method to predict the operating state of the system, and improved the closed-loop stability and economic optimality of the system under the Lyapunov economic predictive control model. On this basis, the prediction model was improved by adding an error-triggering mechanism for prediction errors. The RNN with high prediction accuracy was derived from the latest process data information, and the error-triggering mechanism added would remind the prediction model of dynamic updates in real-time. This prediction model with dynamic performance had certain effectiveness in real-time prediction of practical problems. In addition to RNN, Chen et al. [9] also conducted research on ELM for NLD equations based on machine learning methods, designing a new fault state monitoring model that utilizes improved auto-regressive ELM. The analysis of the NLD relationship of time series data samples by the detection model came from the nonlinear mapping of each data vector. The core principle of fault detection for NLD state was to detect whether the system state is abnormal by detecting the residual between the actual data vector and the corresponding predicted value. Compared with traditional state detection methods, this new model reduced the computational complexity during training and detection, and improved the efficiency of detection. However, Ouyang [10] believed that although ELM has the characteristics of fast computation speed and strong approximation ability, its nonlinear representation of features is not clear enough when constructing a deep learning network. Therefore, the authors improved the original ELM model by incorporating the low-rank matrix decomposition method into the ELM learning process to extract low-dimensional features. Compared to traditional ELM models, this model could customize the number of dimensions in the hidden layer of the model. This reduced the influence of random factors in the feature learning process and improved the nonlinear state representation performance of features. After comparative experiments on numerical and image datasets, it was found that the model has better performance. The summary table of related work is shown in Table 1.

Table 1: Summary table of related work

Field	Researchers	Research content	Research result	Limitations
Non-linear	Salas A H et al. [5]	Exact expression for the Duffiing oscillator period	Integrability of the cubic fifths-order equation	Assumptions and approximations lead to outcome errors
	Akilli M et al. [6]	Duffing the wavelet scale exponent of the oscillator	Signal detection is 90% in real-time	The effects of noise or signal decay
	Pernel Nguenang et al. [7]	Improve the nonlinear resonance phenomenon	The calculation accuracy can be up to 85%	The dynamic state is strongly influenced by the parameters of the equation
Machine learning algorithm	Wu Z et al. [8]	Model based on RNNs	Reduction in the prediction error by 8%	Model requires substantial computational resources and time
	Chen Y et al. [9]	New fault state monitoring model	Reduce computational load by 10%	Requires high computing resources
	Ouyang T et al. [10]	Improving the ELM algorithm model	Improving the performance of non-linear state representation of features	Decreased interpretability of the model

In summary, experts have conducted many studies on the NLD state of microelectronic devices. Experts optimize the NLDE solving method to improve the accuracy of microelectronic device state detection. Some experts also design new detection models based on machine learning algorithms. However, both optimization of equation solving and machine learning algorithms are faced with the problems of large amounts of computation, slow detection speed and high requirements for model computing ability. How to quickly extract the state features of the system while ensuring recognition accuracy is worth studying.

3 Construction of NLD state identification and detection model for microelectronic devices based on ELM

To solve the problem of accurate identification and detection of NLD states in microelectronic devices, a model based on ELM is constructed. The model is based on the Duffing oscillator and NLD system, which are widely used in Micro-Electro-Mechanical Systems (MEMS). The Duffing oscillator's time-series graph analysis and spectral extraction, combined with the ELM algorithm, can efficiently identify and predict state changes in the MEMS system, including periodic and chaotic states. Additionally, the study includes the design of a Josephson Junction detection model based on the noise precursor phenomenon. Effective detection of the Josephson Junction state is achieved by extracting system state features under the influence of noise and training ELM.

3.1 Design of an accurate identification method of microelectronic device state based on ELM

Duffing oscillators are a common nonlinear dynamical system, are increasingly used in MEMS. They are often used to simulate and study complex dynamical behaviors such as chaos, bifurcation, and periodicity due to their unique bistable properties [11]. The study of Duffing oscillators has become increasingly important due to their key role in miniaturized devices, such as sensors, actuators, and signal processing devices, thanks to the development of MEMS technology. However, identifying and predicting the dynamic behavior of MEMS systems accurately is complex and challenging due to their nonlinear nature. Traditional methods for identification and prediction, such as the Lyapunov exponential map method, are theoretically applicable but difficult to meet the real-time and accuracy requirements of practical MEMS applications due to their high computational complexity and slow convergence [12]. Therefore, the study aims to improve the accuracy and prediction efficiency of the identification of the states of Duffing oscillators in MEMS systems through machine learning algorithms, especially ELM. By combining the ELM algorithm and the noise prior law, the study also aims to improve the detection of nonlinear dynamical states and prediction methods of bifurcated states of Josephson junctions, which are common in MEMS systems. In general, the identification of Duffing oscillator states requires first solving the oscillator model parameters after configuring them to obtain the system time sequence

diagram. Based on the time series diagram, the frequency spectrum can be converted to obtain the state features of the system under different bifurcation parameters. This allows for the extraction of a feature matrix. Then, using the bifurcation features extracted in the previous step, a bifurcation diagram is created to obtain the objective matrix. Then the feature matrix is combined to generate a dataset, which is input into ELM to output the recognition accuracy.

Specifically, this manuscript uses the mathematical model expressed in equation (1) to simulate the oscillator system.

$$\ddot{x} + k\dot{x} - x + x^3 = \gamma\cos(\tau) \tag{1}$$

In equation (1), $\gamma\cos(\tau)$ represents the external force driving signal. k is the damping coefficient. x is the distance at which the electromagnet swings in the oscillator system. The nonlinear restoring force is represented by $-x + x^3$. For equation (1), assuming $\tau = \omega t = z$ and $\frac{dx}{d\tau} = \frac{1}{\omega}\frac{dx}{d\tau} = y$, a system of differential equations described by equation (2) can be obtained.

$$\begin{cases} \dfrac{dx}{d\tau} = wy \\ \dfrac{dy}{d\tau} = w(-ky + x - x^3 + \gamma\cos(z)) \\ \dfrac{dz}{d\tau} = w \end{cases} \tag{2}$$

The 4th-order Runge-Kutta method (4ORK) is used to solve Duffing equation. Supposing there is a set of differential equations expressed by equation (3). The 4ORK method is a classical method for the numerical solution of ordinary differential equations, proposed by the German mathematician Carl Wilhelm Runge and the German mathematician Martin Wilhelm Kutta in the late 19th century. The method is based on interpolating polynomials to approximate the solution of differential equations. It estimates the solution at the next step by calculating the slopes of the four intermediate steps, ensuring high order accuracy and good numerical stability.

$$\begin{cases} x(t_0) = given \\ \dfrac{dx(t)}{dt} = f(x(t), t) \end{cases} \tag{3}$$

The 4ORK based on equation (3) is solved by equation (4) [13].

$$\hat{x}(t_{n+1}) = \hat{x}(t_n) + \frac{\Delta t}{6}(k_1 + 2k_2 + 2k_3 + k_4) \tag{4}$$

In equation (4), k_1, k_2, k_3, and k_4 respectively represent the slopes of function $f(x(t), t)$ at different integration points. The core of 4ORK solution is to recursively iterate from $\hat{x}(t_n)$ to $\hat{x}(t_{n+1})$, which is a single iteration, and then repeat the recursion process to obtain the equation solution.

The time series diagram of the state changes of the Duffing oscillator system is obtained by solving a system of differential equations. The system states are periodic and chaotic states, and the transition between the system states can be obtained by changing the driving signal parameters [14]. Considering that 4ORK is a high-precision and small error NLDE iterative solution method, the differential equation is solved using 4ORK. By defining the Duffing oscillator differential equation in Python and 4ORK, the equation solution can be obtained. This process needs to set the initial values of driving parameter k, damping ratio γ and Angular frequency ω of Duffing equation. The driving parameter is set to 0.2, and the Angular frequency is 1. γ is taken as a variable affected the phase state of the system. Figure 1 shows the timing diagram of the system when γ is taken as 1.5, 1.8, 2.1, and 2.4 (Figures 1(a), 1(b), 1(c), 1(d)), where the system is in a chaotic state when γ is taken as 1.8.

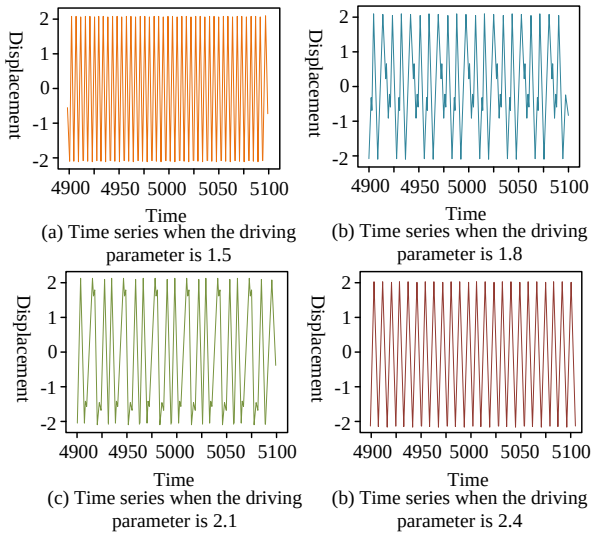

Figure 1: System timing diagram under different driving parameters

The temporal features obtained from Figure 1 are transformed into frequency sequence $F(t)$ through Fourier transform to obtain a frequency spectrum [15]. Figure 2 depicts the frequency changes of the oscillator system under different γ conditions, where each frequency spectrum has several peaks. To generate a feature matrix, the number of peaks in each frequency spectrum is taken as the first feature from Figure 2, and the sum of all peaks is taken as the second feature. These two feature sets for each sample are extracted as a matrix.

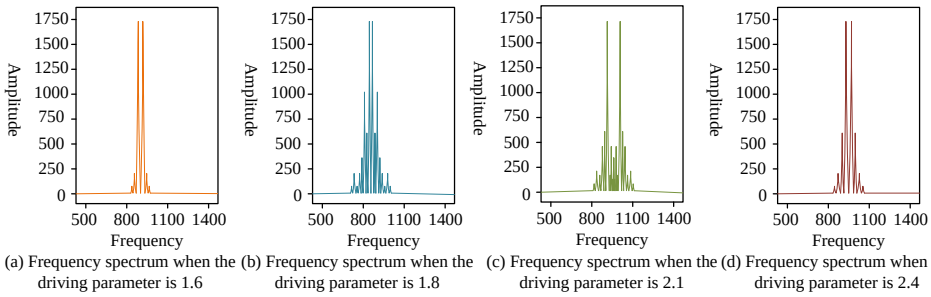

Figure 2: System frequency spectrum under different driving parameters

Assuming there are m samples in total and $n=2$ features in each sample, the feature matrix is set to be $C^{m\times n}$. Firstly, a set of $t_{ia},(a=0,1,...,p_i)$ is extracted by the abscissa corresponding to each peak in the frequency spectrum. p_i is the number of peaks, and i is the i-th sample extracted. For each driving parameter γ_i, the total number of peaks is $P(\gamma_i)$, as described by equation (5).

$$P(\gamma_i)=P_i \tag{5}$$

The first column of the feature matrix $C^{m\times n}$ obtained from equation (5) is calculated by equation (6).

$$C_{i1}=P(\gamma_i),i=0,...,m \tag{6}$$

The second characteristic peak size is represented by $Q(\gamma_i)$ and is described by equation (7).

$$Q(\gamma_i)=\sum\nolimits_a (F(t_{ia})) \tag{7}$$

The second characteristic column of the matrix can be obtained from equation (5), which is calculated by equation (8).

$$C_{i2}=Q(\gamma_i),i=0,...,m \tag{8}$$

The first and second features in feature matrix $C^{m\times n}$ are used as the first and second columns, and the number of rows m is determined by the number of samples. Next, to generate labels for the samples in the feature matrix to obtain the target matrix. Labels will be generated for different periodic and chaotic states in the samples. This study uses the maximum method to create a bifurcation diagram to analyze the state changes of the Duffing system under different γ values. Figure 3 describes the maximum scatter diagram obtained by

solving Duffing equation solving from $\gamma = \gamma_0$ by determining the initial value $\gamma_0 = 1.6$ of γ and the step $\Delta\gamma = 0.0005$, that is, the bifurcation diagram of Duffing equation.

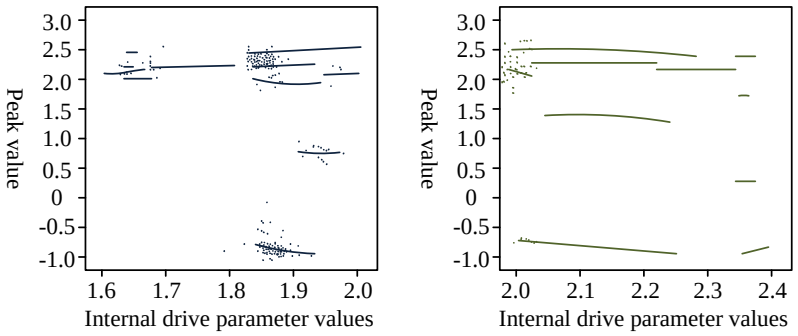

(a) Bifurcation diagram of internal driving parameters in the range of [1.6,2.0]

(b) Bifurcation diagram of internal driving parameters in the range of [2.0,2.4]

Figure 3: Bifurcation diagram of Duffing equation

The system state under each different γ value is extracted from Figure 3 as the row of the objective matrix T, which consists of m rows and 1 column. Next, the objective matrix, feature matrix, and γ are combined to generate dataset D, and finally the dataset is input into ELM to obtain recognition accuracy.

3.2 Design of a josephson junction detection model combining ELM and noise precursor phenomena

Josephson has certain requirements for the stability of the working environment, but there is inevitably noise interference in practical application scenarios. Therefore, it is necessary to be able to detect the working state of the Josephson junction in advance, and adjust the parameters to maintain a stable working state of the Josephson junction for noise interference [16]. This study proposes a detection method for detecting state changes by predicting system bifurcation intervals in the context of ELM and Josephson junction noise precursors.

In general, this detection method first needs to use the Runge–Kutta methods to solve the Josephson junction NLD equation solving in the noise environment. By combining the system state features extracted from the noise precursor phenomenon and inputting them into ELM, nodes that are about to undergo bifurcation in the system will be identified. From this, the operating state of the system can be detected by predicting the bifurcation interval. This paper uses equation (9) to describe the Josephson junction equation.

$$\beta_L\beta_C\ddot{\delta} + \beta_C\dot{\delta} + \dot{\delta}(1 + \beta_L \cos\delta) + \sin\delta = I \quad (9)$$

In equation (9), β_L is the inductance parameter, β_C is the capacitance parameter, and I represents the bias current. $\dot{\delta} = \frac{dx}{dt}$ is proportional to the node voltage in this dimensionless formal equation. Now to let δ be x, $\dot{\delta} = \frac{dx}{dt} = y$, $\ddot{\delta} = \frac{dy}{dt} = z$, $\dddot{\delta} = \frac{dz}{dt}$, and to substitute it into equation (9) to get the Differential form of Josephson junction equation, such as equation (10).

$$\begin{cases} \frac{dx}{dt} = y \\ \frac{dy}{dt} = z \\ \frac{dz}{dt} = \frac{I}{\beta_L\beta_C} - \frac{z}{\beta_L} - \frac{1+\beta_L\cos(x)}{\beta_L\beta_C}y - \frac{\sin(x)}{\beta_L\beta_C} \end{cases} \quad (10)$$

Similar to the Duffing equation, the Josephson junction equation is also solved through 4ORK. Firstly, the inductance parameter in the Josephson junction equation is set to be 3 and the capacitance parameter is 0.1. The bias current I is set as a variable to obtain different system states under different bias currents, and then to create a time series diagram. Figure 4 depicts the timing changes of the system when time t is within the interval [130,150] and the bias current is taken as 5, 6, 7, and 10. The Josephson junction will transition from a multi cycle state to a single cycle state as the bias current increases. The frequency change can be obtained by extracting temporal features from Figure 4 and performing Fourier transform.

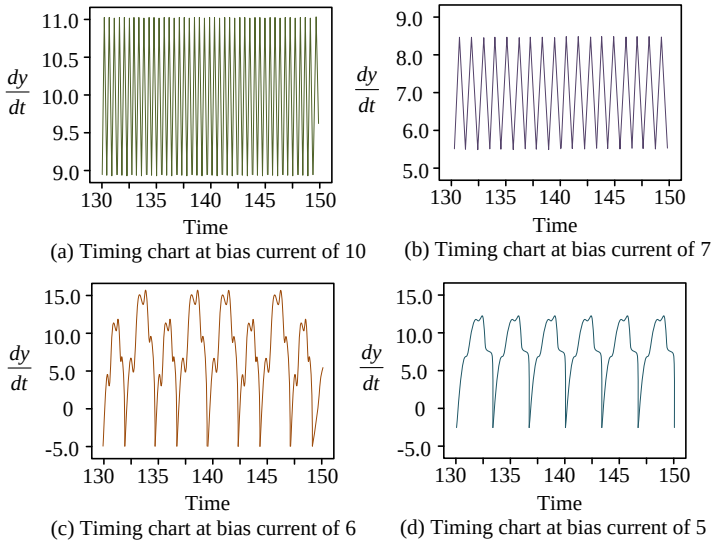

Figure 4: System timing diagram under different bias currents

However, the time series of the bifurcation precursor stage in Figure 4 is similar to the time series of the stable stage and difficult to distinguish, so it is necessary to

extract system state features from the noise precursor phenomenon. When adding random noise to the Josephson junction differential equation, the equation exhibits certain patterns due to continuous changes in bifurcation parameters [17]. Stochastic differential equation is the differential equation under the influence of noise, as equation (11).

$$\frac{dx}{dt} = f(x(t),t) + L(x(t),t)w(t) \tag{11}$$

In equation (11), the system state is represented by $x(t)$, and the input outside the system is represented by $w(t)$. L is the coefficient matrix of $w(t)$, and f is the vector drift rate function [18]. When solving the Stochastic differential equation, it is necessary to give the stochastic Runge–Kutta methods a larger scope of application. Equation (12) is obtained by multiplying both sides of equation (11) by dt.

$$dx = f(x(t),t)dt + L(x(t),t)d\beta \tag{12}$$

In equation (12), $d\beta$ is a Brownian motion increment. At this time, a noise sequence $\beta(t)$ can be represented by m-dimensional standard Brownian motion, as shown in equation (13).

$$\beta(t) = (\beta^{(1)}(t), \beta^{(2)}(t), ..., \beta^{(m)}(t)) \tag{13}$$

The integral form of Stochastic differential equation is obtained from equation (14).

$$x(t) = x(t_0) + \int_{t_0}^{t} f(x(\tau),\tau)d\tau + \int_{t_0}^{t} L(x(\tau),\tau)d\beta(\tau) \tag{14}$$

The Josephson junction equation after adding noise is equation (15).

$$\begin{pmatrix} dx \\ dy \\ dx \end{pmatrix} = \begin{pmatrix} y \\ z \\ \frac{I}{\beta_L\beta_C} - \frac{z}{\beta_L} - \frac{1+\beta_L\cos(x)}{\beta_L\beta_C}y - \frac{\sin(x)}{\beta_L\beta_C} \end{pmatrix} dt + \begin{pmatrix} 0 \\ 0 \\ 1 \end{pmatrix} d\beta \tag{15}$$

After determining the quantities of function $f(x(t),t)$, noise sequence $\beta(t)$, and noise coefficient matrix $L(x(t),t)$, the differential equation can be iteratively solved to obtain a time series diagram under the influence of noise. Similar to Duffing system state recognition, the corresponding frequency spectrum is obtained through Fourier transform. Figure 5 shows the system frequency spectrum of the Josephson junction under the influence of noise, with bias currents of 5, 6, 7, and 10. The system state features are extracted from the spectral changes in Figure 5 to obtain a training dataset. The dataset is then input into the limit state machine for training. By changing the parameters of the system, similar bifurcation points are obtained, and the test set is obtained by analyzing the bifurcation points. Finally, by identifying the test set samples through ELM, the detection results of the Josephson junction state can be obtained.

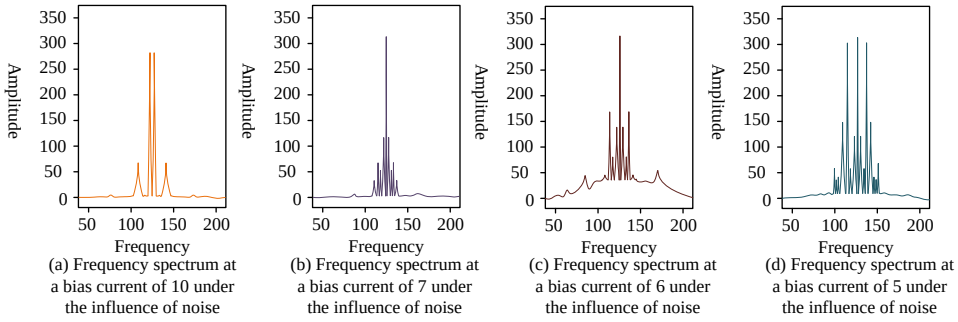

Figure 5: System frequency spectrum under the influence of noise

4 Experimental results and analysis

The third part conducted experimental simulation and result analysis on the identification and detection method based on ELM designed for Duffing oscillator system and Josephson junction. The experiment used Python as the simulation platform, and evaluated the accuracy, running speed, and data volume of ELM under different parameters. RNN algorithm and Lyapunov exponent graph methods were used as a comparison group

4.1 Experimental results and analysis based on duffing oscillator state recognition method

To explore the bifurcation prediction method for the Josephson junction equation based on ELM and noise precursor phenomenon, a two-stage experiment was designed. Firstly, the parameters of the Josephson junction equation were determined, and noise was added to solve it. Secondly, the solved time diagrams were divided into stages, and spectrograms were plotted to generate a training set for training the ELM algorithm. Then, the parameter values in the Josephson junction equation were changed to find new bifurcation points similar to the original bifurcation points, and the test set was generated for testing to obtain the simulation experiment results. The experiment contained four steps: pre-bifurcation stabilization, bifurcation precursor, bifurcation and post-bifurcation stabilization. Finally, the complete training set was generated by extracting the frequency matrix features and extreme point distance features. The set was then trained and tested using the ELM algorithm. Configuring the parameters of the Duffing equation, with a value interval of [1.5, 2.5] for γ and an interval of 0.01, with k taking 0.2 and ω taking 1. 70 random samples out of 100 samples in the dataset are divided as the training set, and the rest as the test set. Feature selection had a significant impact on the performance of ELM models. By selecting appropriate feature subsets, the predictive performance of the model could be improved, the complexity and computational cost of the model could be reduced, and the interpretability of the model could be increased. The experiment used filtering, wrapping, and embedding methods to find the optimal subset of features.

After training, ELM input the test set samples to obtain the output recognition results. By comparing them with the target matrix of the test set, the proportion of samples correctly recognized by ELM in all samples could be determined, which is the accuracy rate. ELM achieved recognition of input data by adjusting the weights of the input and output layers. The details of parameter adjustment included initialization of weights, selection of learning rates, and control of iteration times. The number of hidden layers was an important parameter that affects the performance of ELM. In general, the greater the number of hidden layers in a model, the greater its expressive power. However, this also increased the computational complexity of the model. When processing 1,000 features, 10-20 hidden layers were selected. The activation function was an indispensable part of neural networks, which determined the output range and gradient of the neural network. The experiment used ReLU activation function, which has better performance in processing large-scale datasets. The initialization of weights had a significant impact on the convergence speed and performance of the model. To ensure the convergence of the model, the Xavier initialization method was chosen in the experiment. The learning rate was an important parameter for controlling model updates, and experiments chose different sizes of learning rates such as 0.01, 0.05, and 0.1 for experimentation. The number of iterations was not a fixed parameter 300, rather, it was a variable that determines the adequacy of model training. Table 2 presents the recognition results during the four testing processes: the accuracy of the four recognition results is 90% or above, with a total average accuracy of 93.3%.

Table 2: Identification results during four tests

/	First test	Second test	Third test	Fourth test
Number of samples identified	30	30	29	30

Identify the correct number of samples	27	28	27	30
Total number of samples	30	30	30	30
Accuracy rate	90.0%	93.3%	90.0%	100.0%

Figure 6 compares the detection results of ELM on test samples with the sample labels of the test set during the recognition process. It also included the number of cycles in which each sample state is located. When the number of cycles was 0, the system was in a chaotic state.

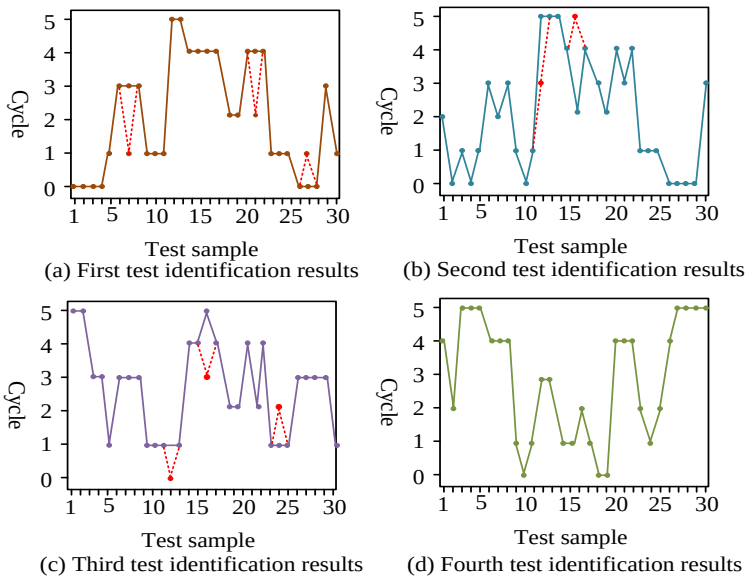

Figure 6: Test results of ELM on samples

Figure 7 compared the operational performance of ELM with RNN and Lyapunov exponent graph methods, with the required amount of data and running time for algorithm operation as evaluation indicators. In Figure 7(a), three samples were not identified accurately with 90% accuracy. Figure 7(b) did not identify one sample with 96.7% accuracy, while Figure 7(c) inaccurately identified four samples with 86.7% accuracy. Figure 7(d) identified all samples with 100% accuracy. Overall comparison showed that after multiple random trials, the average accuracy of state classification for the test samples can reach over 92%. In the whole process from Duffing equation solving to building feature matrix and target matrix to training and recognition test, the running time of ELM was only 70s, which was not at the same level as the time consumed by Lyapunov and RNN. Lyapunov needed to first calculate the maximum Lyapunov exponent to identify the system state, which took 8050s. In contrast, although the running time of RNN was less than half of Lyapunov, it was still two orders of magnitude higher than the ELM. The ELM algorithm required only 80 data points for the recognition process, which was significantly lower than other algorithms that require two to three orders of magnitude.

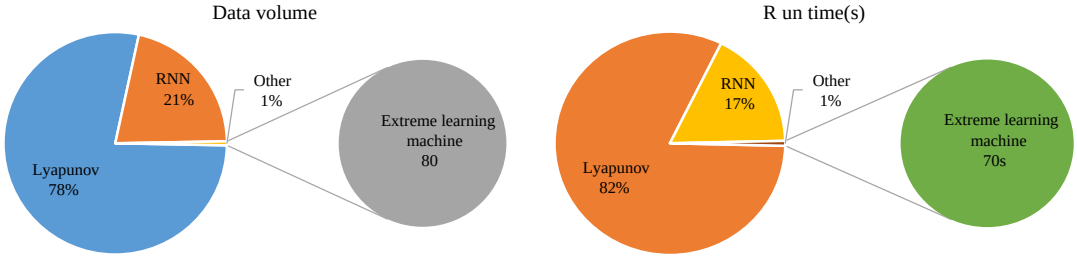

Figure 7: Comparison of operational performance of different algorithms

4.2 Experimental results and analysis of state detection method based on josephson

junction bifurcation stage

The simulation experiment of detecting the Josephson junction state by predicting the bifurcation stage was divided into two stages. In the first stage, experiments were conducted to determine whether accurate predictions could be made for each bifurcation stage. In the second stage, a test set was used to determine whether the method could accurately predict each bifurcation stage for multiple similar bifurcation points. The initial parameters for similar bifurcation points were set as β_L =0.1, β_C =0.07, and the variable bias current I was within the range of [3.5, 5.5]. Figure 8 showed the frequency spectrum of similar bifurcation points at bias currents of 3.7, 4.0, and 4.8. The system was in the post bifurcation stable stage at bias currents of 3.7, 4.0, and 4.8, respectively.

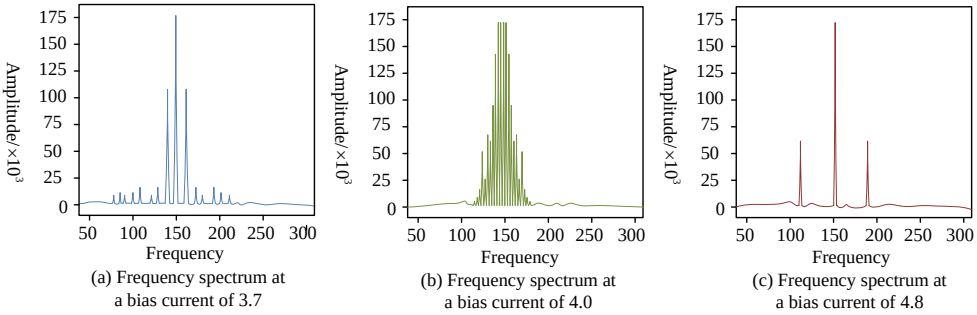

Figure 8: System frequency spectrum under different bias currents

Table 3 presents ELM's accurate predictions for each stage of the bifurcation at this point.

Table 3: Prediction of ELM for each stage of bifurcation

Bias current value range Evaluating indicator	Bifurcation stage	Prediction results of ELM	True or False
[3.7,4.0]	Stable stage after bifurcation	Stable stage after bifurcation	T
[4.0,4.3]	Bifurcation stage	Bifurcation stage	T
[4.3,4.8]	Bifurcation precursor stage	Bifurcation precursor stage	T
[4.8,5.7]	Stability stage before bifurcation	Stability stage before bifurcation	T

After training, ELM input the test set and compared the label matrix of the test set with the obtained detection results for bifurcation points. Table 3 presents the simulation recognition results of ELM in three bifurcation point tests and the comparison results of the target matrix of the test set in the Python environment. In Python, the numbers 0, 1, and 2 were used to refer to the pre bifurcation stage, bifurcation stage, and post bifurcation stable stage, respectively. In Table 4, the accuracy of ELM reached 90% in all three tests of 10 test samples, and reached 100% in the prediction of bifurcation stage and stable stage after bifurcation.

Table 4: Comparison of three test results

First test										
Test set objectives	2	2	2	0	0	0	1	0	1	0
ELM recognition results	2	2	2	1	0	0	1	0	1	0
True or False	T	T	T	F	T	T	T	T	T	T
Second test										
Test set objectives	1	1	1	2	2	2	0	0	0	1
ELM recognition results	1	1	1	2	2	2	2	0	0	1
True or False	T	T	T	T	T	T	F	T	T	T
Third test										
Test set objectives	0	0	0	1	0	1	1	2	2	2
ELM recognition results	0	0	0	1	1	1	1	2	2	2

True or False	T	T	T	T	F	T	T	T	T	T

By changing the parameters to obtain 5 other similar bifurcation points, the test set was input into ELM to obtain the average detection accuracy after 5 tests. Figures 9 (a),(b), (c) compare the accuracy of the ELM algorithm, RNN, and Lyapunov in predicting each of the five bifurcation stages for each of these five bifurcation points. The dashed line in the figure is the average regression line of the algorithm's prediction accuracy for five bifurcation points in each test. In Figure 9, although the prediction accuracy of ELM for each bifurcation point fluctuated slightly by 8 percentage points, the average accuracy of the five tests was above 91%, and the average accuracy was more than 10 percentage points higher than RNN and Lyapunov.

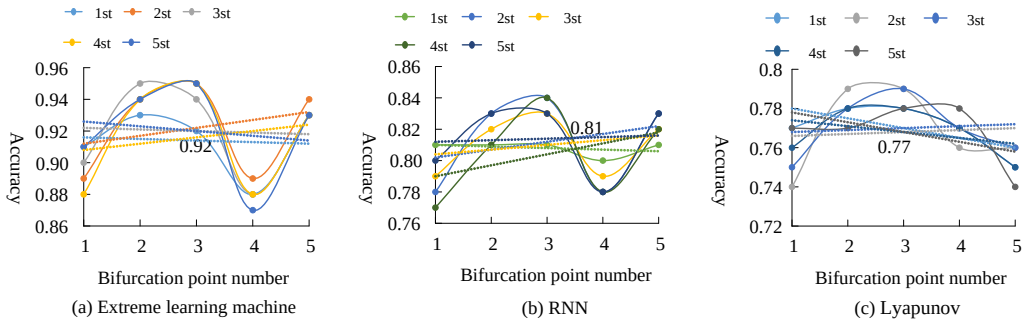

(a) Extreme learning machine (b) RNN (c) Lyapunov

Figure 9: Accuracy comparison in five tests

The precision, recall, and F1 scores of different methods are shown in Table 5. Among the five methods compared, ELM had the highest precision, reaching 93%, followed by the Naive Bayes method with an accuracy of 87%. This indicated that the ELM method had high precision in predicting positive samples. The ELM method had the highest recall rate, reaching 97%. This indicated that the ELM method had a high recall rate in identifying positive samples. The ELM method had the highest F1 score, reaching 94%. This indicated that the ELM method had high accuracy and recall in predicting positive samples, and overall performed the best. ELM performed the best in terms of precision, recall, and F1 score, making it a relatively effective prediction method.

Table 5: Precision, recall and F1-score of different methods

Methods	Precision	Recall	F1-score
ELM	93%	97%	94%
RNN	83%	85%	83%
Lyapunov	80%	84%	81%
Support vector machine	86%	90%	88%
Naive Bayes	87%	92%	90%

4.3 Discussion

The results demonstrate that the Duffing oscillator state recognition method based on ELM and the Josephson junction bifurcation stage state detection method have significant advantages in accuracy, running speed, and data volume. In the Duffing oscillator state recognition experiment, the recognition accuracy of the four ELM tests is above 90%, with a total average accuracy of 93.3%. In contrast, the runtime of RNN algorithm and Lyapunov exponent graph method is two orders of magnitude higher than ELM and three orders of magnitude higher, respectively, and ELM also has relatively low requirements for data volume. In the Josephson junction bifurcation stage state detection experiment, ELM achieves an accuracy of 90% in all 10 test samples, and an accuracy of 100% in predicting bifurcation stage and stable stage after bifurcation. In addition, ELM performs the best in terms of accuracy, recall, and F1 score, making it a more effective prediction method.

By comparing with the most advanced methods currently available, it can be found that ELM has significant advantages in certain aspects. This is mainly attributed to the superiority of ELM in parameter adjustment, feature selection, and model interpretability. Firstly, ELM can recognize input data by adjusting the weights of the input and output layers, thereby achieving high recognition accuracy under different parameters [19]. Secondly, by using feature selection methods such as filtering, wrapping, and embedding, ELM can find the optimal subset of features, further improving the predictive performance and interpretability of the model [20]. In addition, the running speed and data volume requirements of ELM are relatively low, making it more efficient in practical applications. However, ELM may perform poorly in certain situations. When the system is in a chaotic state, the recognition accuracy of ELM will

decrease. This is because the nonlinear characteristics of the system in chaotic states can make it difficult for ELM to capture effective features. Furthermore, it is possible that ELM may be susceptible to overfitting when processing large amounts of data. In such instances, it may be necessary to optimize the model through regularization and other methods.

5 Conclusion

In microelectronic device research and development, it is crucial to accurately identify and predict the nonlinear dynamical states of the devices to ensure their performance and reliability. The Duffing vibrator system is one of many NLD models that has received special attention due to its wide application in microelectronic devices. The traditional state recognition method of Duffing oscillator system has the problems of large computation, slow rate of convergence and limited recognition accuracy. The traditional bifurcation prediction method of Josephson junction also has the problem of inaccurate extraction of bifurcation characteristics. Therefore, this paper proposed the Duffing oscillator system identification method based on ELM and a new bifurcation prediction method combining the noise precursor law of Josephson junction with ELM. The results demonstrated that the accuracy of the four recognition results of ELM in Duffing oscillator system state recognition for the training set samples was 90% or above, with a total average accuracy of 93.3%. In comparison experiments with traditional Lyapunov exponent graph method and RNN algorithm, ELM had a requirement of 80 bytes of data and a recognition process running time of 70s, both of which were two to three orders of magnitude smaller than traditional algorithms. The detection results of the bifurcation state of the Josephson junction indicated that the ELM accuracy reached 100% in the prediction of the first similar bifurcation point at each stage. The accuracy rate reached 90% during the three tests on the test set samples, and reached 100% during the predicted bifurcation stage and post bifurcation stable stage. In the five-test detection of five similar bifurcation points, the prediction accuracy of ELM for different bifurcation points fluctuated slightly within 8 percentage points. The average accuracy of the five tests was above 91%, with a maximum of 95%, and the average accuracy was more than 10 percentage points higher than traditional detection algorithms. The paper presents improved identification and detection methods for Duffing oscillators and Josephson junctions. Nevertheless, the applicability of the ELM algorithm is constrained by the complexity of the problem and the characteristics of the data, and it may not perform optimally in other contexts. The interpretation of algorithmic data is based on specific conditions and metrics that may not be robust under other experimental conditions. Additionally, the study only considers the most common noise precursor law of Josephson junctions. In different bifurcation modes, the characteristics of noise precursor phenomena are different, which is also a direction that can be studied in the future. Meanwhile, in the study of the Duffing system, there are other methods of extracting features through phase diagrams. Adding more features to the dataset can effectively improve the accuracy of the ELM.

6 Statements and declarations

Competing Interests: The authors have no relevant financial or non-financial interests to disclose.

Funding: No funding was received for conducting this study.

References

[1] Z. Wang, H. Chen, and Y. Tang, “The focus case of a nonsmooth Rayleigh-duffing oscillator,” Nonlinear Dynamics, vol. 107 no. 1, pp. 269-311, 2022. https://doi.org/10.1007/s11071-021-07007-9

[2] A. H. Salas, S. A. El-Tantawy, and N. H. Aljahdaly, “An exact solution to the quadratic damping strong nonlinearity duffing oscillator,” Mathematical Problems in Engineering, vol. 2021 no. 13, pp. 1-8, 2021. https://doi.org/10.1155/2021/8875589

[3] S. Roy, D. Das, and D. Banerjee, “Vibrational resonance in a bistable van der Pol-Mathieu-Duffing oscillator,” International Journal of Non-Linear Mechanics, vol. 135 no. 6, pp. 103771, 2021. https://doi.org/10.1016/j.ijnonlinmec.2021.103771

[4] A. H. S. Salas, J. E. C. Hernández, and L. J. M. Hernández, “The duffing oscillator equation and its applications in physics,” Mathematical Problems in Engineering, vol. 2021, pp. 9994967, 2021. https://doi.org/10.1155/2021/9994967

[5] A. H. Salas and S. C. Trujillo, “A new approach for solving the complex cubic-quintic duffing oscillator equation for given arbitrary initial conditions,” Mathematical Problems in Engineering, vol. 2020, pp. 3985975, 2020. https://doi.org/10.1155/2020/3985975

[6] M. Akilli, N. Yilmaz, and K. G. Akdeniz, “Automated system for weak periodic signal detection based on Duffing oscillator,” IET Signal Processing, vol. 14 no. 3, pp. 710-716, 2021. https://doi.org/10.1049/iet-spr.2020.0203

[7] N. Pernel, T. M. Sandrine, L. Patrick, A. T. Tsokeng, and M. Tchoffo, “Nonlinear resonances phenomena in a modified Josephson junction model,” Chinese Physics B, vol. 29 no. 12, pp. 197-208, 2020. https://doi.org/10.1088/1674-1056/aba9cd

[8] Z. Wu, D. Rincon, and P. D. Christofides, “Real-time adaptive machine-learning-based predictive control of nonlinear processes,” Industrial and Engineering Chemistry Research, vol. 59 no. 6, pp. 2275-2290, 2020. https://doi.org/10.1021/acs.iecr.9b03055

[9] Y. Chen, C. Tong, Y. Ge, and T. Lan, “Fault detection based on auto-regressive extreme learning machine

for nonlinear dynamic processes," Applied Soft Computing, vol. 106 no. 8, pp. 107319, 2021. https://doi.org/10.1016/j.asoc.2021.107319

[10] T. Ouyang, "Feature learning for stacked elm via low-rank matrix factorization," Neurocomputing, vol. 448, pp. 82-93, 2021. https://doi.org/10.1016/j.neucom.2021.03.110

[11] M. J. Brennan, G. Gatti, and I. Kovacic, "On rotating vectors, Jacobi elliptic functions and free vibration of the Duffing oscillator," International Journal of Non-Linear Mechanics, vol. 126, pp. 103566., 2020. https://doi.org/10.1016/j.ijnonlinmec.2020.103566

[12] I. N. Askerzade and R. Askerbeyli, "Return current of dc SQUID based on tunnel Josephson junctions with unconventional current-phase relation," Low Temperature Physics, vol. 47 no. 5, pp. 424-428, 2021. https://doi.org/10.1063/10.0004232

[13] H. Wang, R. S. Deacon, and K. Ishibashi, "Bismuth nanowires with in situ shadow deposited Josephson junctions," Applied Physics Letters, vol. 121 no. 8, pp. 083503, 2022. https://doi.org/10.1063/5.0101454

[14] E. Neumann and A. Pikovsky, "Quasiperiodically driven Josephson junctions: strange nonchaotic attractors, symmetries and transport," European Physical Journal, B, vol. 26 no. 2, pp. 219-228, 2021. https://doi.org/10.1140/EPJB/E20020083

[15] N. Raza, M. Tahir, and K. Ali, "Sparse extreme learning machine," Electronics Letters, vol. 56 no. 23, pp. 1277-1280, 2020. https://doi.org/10.1049/el.2020.1840

[16] M. Cuzminschi and A. Zubarev, "Chaotic behavior of a stack of intrinsic Josephson junctions at the transition to branching for overcritical currents," Chinese Journal of Physics, vol. 71, pp. 634-642, 2021. https://doi.org/10.1016/j.cjph.2021.03.025

[17] I. N. Askerzade and A. Aydin, "Frustration effect on escape rate in Josephson junctions between single-band and three-band superconductors in the macroscopic quantum tunneling regime," Low Temperature Physics, vol. 47 no. 4, pp. 282-286, 2021. https://doi.org/10.1063/10.0003738

[18] T. Yamashita, "Magnetic Josephson junctions: new phenomena and physics with diluted alloy, conventional ferromagnet, and multilayer barriers," IEICE Transactions on Electronics, vol. E104/C, no. 9, pp. 422-428, 2021. https://doi.org/10.1587/transele.2020SUI0004

[19] Y. Guo, Z. Mustafaoglu, and D. Koundal, "Spam detection using bidirectional transformers and machine learning classifier algorithms," Journal of Computational and Cognitive Engineering, vol. 2, no. 1, pp. 5-9, 2022. https://doi.org/10.47852/bonviewJCCE2202192

[20] L. Li, "Dynamic Cost Estimation of Reconstruction Project Based on Particle Swarm Optimization Algorithm," Informatica, vol. 47, no. 2, pp. 173-182, 2023. https://doi.org/10.31449/inf.v47i2.4026